Miner Petrol (2009) 96:221–232
DOI 10.1007/s00710-009-0050-9

ORIGINAL PAPER

Friedrichbeckeite, K $(\square_{0.5}Na_{0.5})_2$ $(Mg_{0.8}Mn_{0.1}Fe_{0.1})_2$ $(Be_{0.6}\ Mg_{0.4})_3$ $[Si_{12}O_{30}]$, a new milarite-type mineral from the Bellerberg volcano, Eifel area, Germany

C. L. Lengauer · N. Hrauda · U. Kolitsch · R. Krickl · E. Tillmanns

Received: 16 October 2008 / Accepted: 17 March 2009 / Published online: 8 May 2009

Abstract Friedrichbeckeite is a new milarite-type mineral. It was found in a single silicate-rich xenolith from a quarry at the Bellerberg volcano near Ettringen, eastern Eifel volcanic area, Germany. It forms thin tabular crystals flattened on {0001}, with a maximum diameter of 0.6 mm and a maximum thickness of 0.1 mm. It is associated with quartz, tridymite, augite, sanidine, magnesiohornblende, enstatite, pyrope, fluorapatite, hematite, braunite and roeddderite. Friedrichbeckeite is light yellow, with white to light cream streak and vitreous lustre. It is brittle with irregular fracture and no cleavage, Mohs hardness of 6, calculated density is 2.686 gcm^{-3}. Optically, it is uniaxial positive with n_ω = 1.552(2) and n_ε = 1.561(2) at 589.3 nm and a distinct pleochroism from yellow (//ω) to light blue (//ε). Electron microprobe analyses yielded (wt.%): Na_2O 2.73, K_2O 4.16, BeO 4.67, MgO 11.24, MnO 2.05, FeO 1.76, Al_2O_3 0.15, SiO_2 73.51, (Σ CaO, TiO_2 = 0.06) sum 100.33 (BeO determined by LA-ICP-MS). The empirical formula based on Si = 12 is $K_{0.87}$ $Na_{0.86}$ $(Mg_{1.57}Mn_{0.28}Fe_{0.24})_{\Sigma 2.09}$ $(Be_{1.83}Mg_{1.17})_{\Sigma 3.00}$ $[Si_{12}O_{30}]$, and the simplified formula can be given as K $(\square_{0.5}Na_{0.5})_2$ $(Mg_{0.8}Mn_{0.1}Fe_{0.1})_2$ $(Be_{0.6}$ $Mg_{0.4})_3$ $[Si_{12}O_{30}]$. Friedrichbeckeite is hexagonal, space-group *P6/mcc*, with *a* = 9.970(1), *c* = 14.130(3) Å, *V* = 1216.4(3) $Å^3$, and *Z* = 2. The strongest lines in the X-ray powder diffraction pattern are (*d* in Å / I_{obs} / *hkl*): 3.180 / 100 / 121, 2.885 / 70 / 114, 4.993 / 30 / 110, 4.081 / 30 / 112, 3.690 / 30 / 022. A single-crystal structure refinement (*R*1 = 3.62 %) confirmed that the structure is isotypic with milarite and related $^{[12]}C$ $^{[9]}B_2$ $^{[6]}A_2$ $^{[4]}T2_3$ $[^{[4]}T1_{12}O_{30}]$ compounds. The *C*-site is dominated by potassium, the *B*-site is almost half occupied by sodium, and the *A*-site is dominated by Mg. The site-scattering at the *T*2-site can be refined to a Be/(Be+Mg) value close to 0.61; the *T*1-site is occupied by Si. Micro-Raman spectroscopy reveals an increasing splitting of scattering bands around 550 cm^{-1} for friedrichbeckeite. The mineral can be classified as an unbranched ring silicate or as a beryllo-magnesiosilicate. With respect to the end-member formula K $(\square 0.5Na0.5)_2$ Mg_2 Be_3 $[Si_{12}O_{30}]$ friedrichbeckeite represents the Mg-dominant analogue of almarudite, milarite or oftedalite. The mineral and its paragenesis were formed during pyrometamorphic modifications of the silicate-rich xenoliths enclosed in Quaternary leucite-tephritic lava of the Bellerberg volcano. Holotype material of friedrichbeckeite has been deposited at the mineral collection of the Naturhistorisches Museum Wien, Austria. The mineral is named friedrichbeckeite in honour of the Austrian mineralogist and petrographer Friedrich Johann Karl Becke (1855–1931).

Editorial handling: A. R. Chakhmouradian

C. L. Lengauer (✉) · R. Krickl · E. Tillmanns
Institut für Mineralogie und Kristallographie,
Universität Wien-Geozentrum,
Althanstrasse 14,
A-1090 Wien, Austria
e-mail: christian.lengauer@univie.ac.at

N. Hrauda
Institut für Halbleiter- und Festkörperphysik,
Johannes Keppler Universität Linz,
Linz, Austria

U. Kolitsch
Mineralogisch-Petrographische Abteilung,
Naturhistorisches Museum,
Wien, Austria

Introduction

This article describes the new mineral species friedrichbeckeite, found in a xenolith from the Bellerberg volcano

SE of Ettringen, Germany, which is located within the region around the Laacher See and is part of the Quaternary East Eifel volcanic area. The Bellerberg volcano (rarely also named Bellberg or Bell-Berg), is a remnant of volcanic activity during the late Wehrer eruptive phase (Bogaard and Schmincke 1990: 150–100 ka). It is a locality famous for uncommon and new mineral species formed due to the pyrometamorphic interaction of silicate- or calcium-rich xenoliths with a leucite-tephritic lava (e.g. Abraham et al. 1983; Krause et al. 1999) and subsequent metasomatic alterations (e.g. Rüdinger et al. 1993; Irran et al. 1997). The geology and mineralogy of this locality were discussed and compiled by Meyer (1994) and Hentschel (1987), respectively.

The mineral at the focus of this study is a new magnesium-rich and beryllium-bearing member of the milarite- or osumilite-type minerals, discussed in detail by Forbes et al. (1972), Černý et al. (1980) and Hawthorne et al. (1991). These authors established the general structural formula of milarite-group minerals: $^{[18]}D\ ^{[12]}C\ ^{[9]}B_2\ ^{[6]}A_2\ ^{[4]}T2_3\ [^{[4]}T1_{12}O_{30}]$, where D = □ or H_2O; C = □, Na, K or Ba; B = □, Na, K or H_2O; A = Na, Mg, Ca, Sc, Ti, Mn, Fe or Zr; $T2$ = Li, Be, B, Mg, Al, Si, Mn, Fe or Zn, $T1$ = Al or Si. Based on this crystal-chemical versatility, high temperature stability and low thermal expansion coefficients, the magnesium- and aluminium-rich osumilite-type compounds are of special interest in glass ceramic applications (Winter et al. 1993, 1995). Up to now, however, no synthetic analogue of friedrichbeckeite has been known and it is the second finding of a Be-bearing mineral in the volcanic rocks of the Eifel region after the isotypic mineral almarudite (Mihajlović et al. 2004).The occurrence and paragenesis of friedrichbeckeite are similar to those of the other previously reported isotypic minerals eifelite, roedderite, osumilite and osumilite-(Mg), also found in silicate-rich xenoliths at the Bellerberg (Hentschel 1987).

Friedrichbeckeite was found in a suite of xenolithic sample materials collected and kindly provided by Joachim Jahn, Neuwied, Germany. The mineral is named in honour of the Austrian mineralogist and petrographer Friedrich Johann Karl Becke (1855–1931), who served as Head of the Mineralogisch-Petrographisches Institut at the Universität Wien from 1898 to 1927 and is best known for developing the central illumination technique, called the Becke-line method (Becke 1892). Before this work Friedrich Becke was choosen as the namesake for beckelite, which was discredited as material identical to britholite-(Ce) (Embrey and Fuller 1980). The name friedrichbeckeite was preferred to the shorter name beckeite to avoid confusion with beckit (or beekite), which refers to corals and shells pseudomorphed by chalcedony (Chester 1896).

Both the mineral and its name were approved by the International Mineralogical Association Commission on New Minerals, Nomenclature and Classification (IMA 2008–19). The investigated holotype as well as cotype material are preserved at the mineral collection of the Naturhistorisches Museum Wien (NHMW), Austria, with catalogue number 2009–IV-a.

Occurrence and paragenesis

The investigated material was found in the quarry of the firm ‘A. Caspar’ within the Bellerberg volcano (N 50° 21′ 9″ E 7° 14′ 3″). In common with the other previously mentioned occurrences of milarite-type minerals, friedrichbeckeite occurs in vesicles of pyrometamorphically modified silicate-rich xenoliths of Variscan basement enclosed in the leucite-tephritic lava. The mineral has crystallized from Mg- and Si-rich gas phases generated by reaction of gaseous differentiates with the xenolith material (Schreyer et al. 1983). The bulk of the xenolith is composed of a white to light yellow aggregate of quartz and sanidine. Other associated minerals include thin platelets of tridymite, augite, magnesiohornblende, enstatite, almandine-spessartine garnet, acicular fluorapatite, biotite, dipyramidal crystals of braunite and rhombohedral crystals of Ti-Mn-bearing hematite twinned on $10\bar{1}0$ as well as Mn-bearing roedderite, $K(Na_{0.5}\square_{0.5})_2Mg_2(Mg_{0.8}Mn_{0.2})_3[Si_{12}O_{30}]$. The roedderite occurs either as clear columnar crystals or as thick tabular forms with oriented, lamellar inclusions of ilmenite and quartz (Hrauda 2006). Additionally, mullite, cordierite, powellite, bixbyite and rhönite are known from similar parageneses (Hentschel 1987).

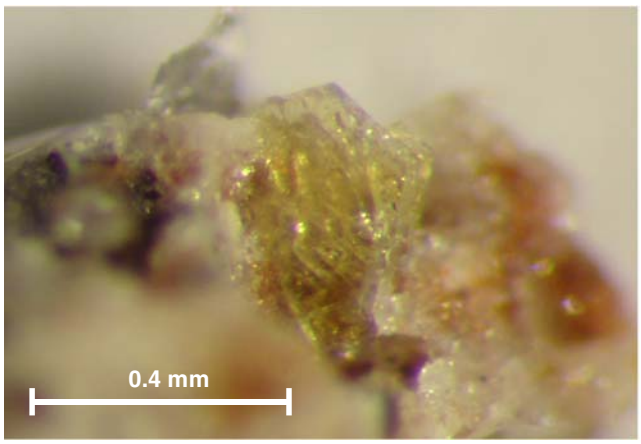

Fig. 1 Microphotograph of co-type friedrichbeckeite from the Bellerberg, Eifel, Germany, showing the light yellow colour and the typical tabular habit, flattened on {0001}

Appearance and physical properties

Friedrichbeckeite forms euhedral, thin tabular crystals flattened on {0001}, with a maximum diameter of 0.6 mm and a thickness of up to 0.1 mm (Fig. 1). In addition to the dominant {0001} pinacoid face, the crystals exhibit $\{10\bar{1}0\}$ and, less common $\{11\bar{2}0\}$ faces. Twinning is not observed. The mineral is colourless to light yellow, has a colourless to light cream streak and vitreous lustre. Tenacity is brittle with irregular fracture, no cleavage or parting is observed. The Mohs hardness is 6, the calculated density from empirical chemical formula and single-crystal unit-cell parameters is 2.686 gcm^{-3}. Friedrichbeckeite fragments were mounted on glass fibres and inspected under a polarizing microscope equipped with a spindle stage. The mineral is uniaxial positive with n_ω = 1.552(2) and n_ε = 1.561(2) at 589.3 nm and 297 K; however, anomalous extinction, subtle biaxiality and zoning are sometimes present. The same features were also reported for osumilite (Schreyer et al. 1983) and almarudite (Mihajlović et al. 2004), the optically negative Mn-analogue of friedrichbeckeite. The pleochroism is distinct from yellow (//ω) to light blue (//ε). The compatibility index, calculated from the Gladstone-Dale relationship (Mandarino 1981), is 0.002 (superior).

Chemical composition

The chemical composition of friedrichbeckeite (Table 1) was determined by wavelength-dispersive electron microprobe (EMP) analysis, which was performed on a Cameca SX100 instrument at 15 kV, 20 nA sample current, with the beam diameter < 1 μm and measurement time of 20 s per element. The Be-content was measured by laser-ablation inductively coupled plasma mass spectrometry (LA-ICP-MS) using the New Wave 193 nm pulsed solid state laser system (beam diameter ~ 20 μm) under helium atmosphere (purity 6.0), and a Nu high-resolution multi-collector ICP-MS with argon gas (purity 6.0) as the transport medium. Lithium and boron were sought for, but not found to be present at detectable levels (50 and 80 ppm, respectively). The results of the chemical analyses as well as the used standard materials are listed in Table 1.

Using the general structural formula of the milarite-type compounds $^{[12]}C\ ^{[9]}B_2\ ^{[6]}A_2\ ^{[4]}T2_3\ [^{[4]}T1_{12}O_{30}]$, the empirical formula obtained from the EMP and LA-ICP-MS analyses calculated on the basis of Si = 12 is $K_{0.87}\ Na_{0.86}\ (Mg_{1.57}Mn_{0.28}Fe_{0.24})_{\Sigma 2.09}\ (Be_{1.83}Mg_{1.17})_{\Sigma 3.00}\ [Si_{12}O_{30}]$, which can be simplified to $K\ (\square_{0.5}Na_{0.5})_2\ (Mg_{0.8}Mn_{0.1}Fe_{0.1})_2\ (Be_{0.6}Mg_{0.4})_3\ [Si_{12}O_{30}]$. The end-member formula can be given as $K\ (\square 0.5Na0.5)_2\ Mg_2\ Be_3\ [Si_{12}O_{30}]$.

In contrast to the values given for milarite (Al_2O_3: 3.3–7.0, CaO: 9.3–11.6 wt%) by Hawthorne et al. (1991), friedrichbeckeite contains almost no CaO (0.04 wt%) and Al_2O_3 (0.15 wt%). By comparison to almarudite (MgO: 1.5, MnO: 7.3, FeO: 4.5 wt% by Mihajlović et al. 2004) it contains much more MgO (11.24 wt%) and significantly less MnO (2.05 wt%) and FeO (1.76 wt%). It is worth noting that only trace amounts of TiO_2, close to the detection limit of the EMP system, were observed. As indicated by the optical observations (Fig. 1) the chemical analyses of the investigated crystals confirm the zoning to be due to chemical variations in the octahedrally coordinated *A*-site with the Mg ↔ Mn > Fe substitution at the outer rim. Water is not present in friedrichbeckeite in amounts detectable by Micro-Raman spectroscopy (see below), which is consistent with the pyrometamorphic origin of this milarite-type mineral.

Powder X-ray diffractometry

The X-ray powder diffraction data for friedrichbeckeite (Table 2) were obtained with a 114.59 mm Debye-Scherrer camera equipped with a Gandolfi attachment (Gandolfi

Table 1 Chemical composition of friedrichbeckeite (wt.%)

Oxide	Mean	Range	S.D.	Calculated	Standard
Na_2O[a]	2.73	2.43–3.04	0.19	3.19	albite
K_2O[a]	4.16	4.10–4.25	0.04	4.86	orthoclase
BeO[b]	4.67	4.26–5.72	0.73	5.16	beryl
MgO[a]	11.24	9.19–12.71	1.22	12.46	olivine
CaO[a]	0.04	0.01–0.10	0.03		periclase syn.
MnO[a]	2.05	1.70–2.55	0.30		spessartine
FeO[a]	1.76	1.20–2.24	0.41		wuestite syn.
Al_2O_3[a]	0.15	0.08–0.19	0.04		corundum syn.
SiO_2[a]	73.51	72.96–74.43	0.43	74.33	quartz syn.
TiO_2[a]	0.02	0.00–0.04	0.01		rutile syn.
Total	100.33			100.00	

Calculated: required chemical composition of the end-member $K\ (\square_{0.5}Na_{0.5})_2\ Mg_2\ Be_3\ [Si_{12}O_{30}]$

[a] from 15 EMP analyses of three grains, [b] from 5 LA-ICP-MS analyses

1964) in asymmetric setting (Straumanis and Jevinš 1936) using Ni-filtered CuK_α radiation (30 kV, 30 mA) and exposure time of 16 h. Data were corrected for film shrinkage, the I_{obs} values were estimated visually, *hkl* assignments were based on a theoretical powder pattern calculated from the refined structure model (Fischer et al. 1993), and the unit-cell parameters were obtained using software NBS*AIDS83 (Mighell et al. 1981). The calculated powder pattern as well as the corresponding part of the Gandolfi film is shown in Fig. 2. The refined hexagonal unit-cell parameters for friedrichbeckeite (a = 9.975(2), c = 14.134(2) Å) compare well with those obtained from

Table 2 X-ray powder diffraction data for friedrichbeckeite

I_{obs}	I_{calc}	d_{obs}	d_{calc}	h	k	l
10	15.6	7.057	7.0670	0	0	2
5	4.7	5.459	5.4699	0	1	2
30	30.0	4.993	4.9875	1	1	0
25	19.7	4.321	4.3193	0	2	0
30	37.0	4.081	4.0749	1	1	2
30	26.0	3.690	3.6854	0	2	2
25	24.8	3.525	3.5335	0	0	4
10	13.8	3.274	3.2705	0	1	4
	3.6		3.2651	1	2	0
100	100.0	3.180	3.1813	1	2	1
70	62.9	2.885	2.8832	1	1	4
	7.1		2.8795	0	3	0
25	30.1	2.737	2.7349	0	2	4
5	10.7	2.686	2.6836	1	2	3
10	8.6	2.495	2.4938	2	2	0
5	7.7	2.397	2.3959	1	3	0
5	2.6	2.362	2.3622	1	3	1
5	2.2	2.273	2.2727	0	1	6
	1.2		2.2691	1	3	2
5	7.0	2.135	2.1356	1	3	3
5	1.7	2.066	2.0654	0	4	2
5	9.6	1.984	1.9830	1	3	4
	2.6		1.9818	2	3	0
5	10.7	1.869	1.8686	1	4	1
15	16.9	1.828	1.8277	1	3	5
	5.1		1.8233	0	3	6
5	7.3	1.766	1.7668	0	0	8
5	5.6	1.727	1.7277	0	5	0
5	10.3	1.712	1.7124	2	2	6
5	5.1	1.664	1.6632	1	4	4
	2.0		1.6625	3	3	0
5	2.8	1.636	1.6352	0	2	8
5	4.3	1.568	1.5684	1	4	5
5	1.3	1.543	1.5426	2	4	3
	2.4		1.5423	1	5	1
5	4.0	1.505	1.5059	0	3	8
	6.6		1.5043	3	3	4
5	2.1	1.474	1.4737	1	5	3
5	6.8	1.442	1.4416	2	2	8
5	4.3	1.414	1.4137	2	4	5
5	9.6	1.383	1.3833	2	5	0
5	2.9	1.359	1.3599	1	1	10
5	5.0	1.333	1.3333	0	6	4
5	7.6	1.314	1.3134	1	3	9
5	3.4	1.288	1.2881	2	5	4
5	3.7	1.193	1.1928	2	5	6
5	4.5	1.176	1.1758	4	4	4
5	4.5	1.089	1.0892	2	5	8

Experimental: Debye-Scherrer camera equipped with a Gandolfi attachment, diameter 114.59 mm, Cu$K\alpha$, Ni-filter, 16 h, I_{obs} estimated visually, I_{calc} and *hkl* indexing based on a theoretical powder pattern calculated from the refined single-crystal structure, d_{calc} derived from the refined unit-cell parameters of the powder data with a = 9.975(2) Å and c = 14.134(4) Å

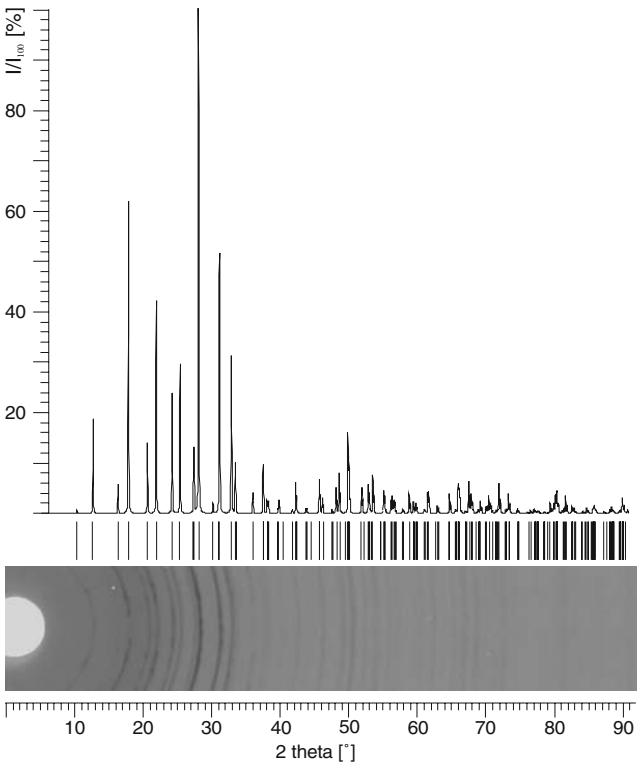

Fig. 2 Simulated powder X-ray diffraction pattern of friedrichbeckeite for Bragg-Brentano geometry and Cu$K\alpha$ radiation using the positional and isotropic displacement parameters of the single-crystal refinement (*upper curve*), the calculated peak positions (*vertical tick marks*), and the corresponding section of the Gandolfi film

Table 3 Single-crystal X-ray data collection and structure refinement of friedrichbeckeite

Space-group	*P6/mcc*, no. 192	Equipment	Nonius KappaCCD
Z	2	θ range (°)	3.73–30.49
a (Å)	9.970(1)	*h*, *k*, *l* ranges	$-14<h<14$
c (Å)	14.130(3)		$-11<k<11$
V (Å^3)	1216.4(3)		$-20<l<20$
D_{calc} (gcm^{-3})	2.686	No. of F_o^2 in Ewald sphere	5919
Formula weight	983.69		
Wavelength (Å)	0.71073	No. of unique F_o^2	644 (R_{int} 2.43 %)
μ MoK_α (cm^{-1})	1.294	No. of $F_o^2 > 2\sigma(F_o^2)$	586
Crystal size (mm)	0.05×0.07×0.08	No. of parameters	51
Transmission factors	0.903–0.938	No. of constraints	2
Absorption correction	multi-scan	*R*1, $R1 > 2\sigma(F_o^2)$	3.62, 3.12 %
		w*R*2, $wR2 > 2\sigma(F_o^2)$	8.82, 8.39 %
		GOF, Δ_{max}/σ	1.165, 0.007
		Δ eÅ^{-3}min, max	−0.32, 0.55

$R1 = \Sigma(\left|\left|F_o\right|-\left|F_c\right|\right|) / \Sigma\left|F_o\right|$, $wR2 = [\Sigma\, w(F_o^2 - F_c^2)^2 / \Sigma\, w(F_o^2)^2]^{1/2}$, GOF = $\{\Sigma\, [w(F_o^2 - F_c^2)^2] / (n-p)\}^{1/2}$, n=644, p=51, $w = 1 / [\sigma^2 F_o^2 + (a\times P)^2 + b \times P]$, a=0.05, b=1.15, $P=[\max(F_o^2,0) + 2 \times F_c^2] / 3$

the single-crystal data (Table 3). For both methods, the calculated *c*:*a* ratio is 1.417. Due to their higher accuracy, the unit-cell parameters obtained from the single-crystal study were used for structure refinements and subsequent crystal-chemical calculations.

Micro-Raman spectroscopy

Raman spectroscopic investigations were performed using a Renishaw RM1000 spectrometer equipped with an edge-filter system, a single monochromator with a grating of 1,200 grooves per mm and a Peltier-cooled CCD detector, attached to a Leica DMLM microscope. Spectra were excited by the 633 nm emission of a He-Ne laser (17 mW). Wavenumber accuracy, calibrated using the Rayleigh line and the Ne lamp emissions, was 0.5 cm^{-1} and the spectral resolution was determined to be 1 cm^{-1}. For comparative purposes, Raman spectra of friedrichbeckeite, almarudite and milarite were recorded in the range 1,400–50 cm^{-1} and are shown in Fig. 3.

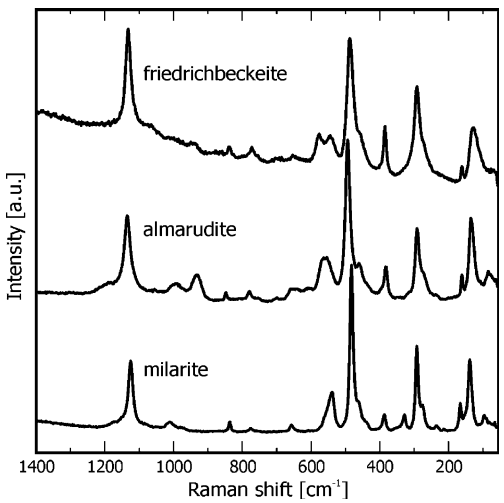

Fig. 3 Micro-Raman spectra (633 nm excitation) along [0001] of holotype friedrichbeckeite, holotype almarudite and a milarite from Rössing, Namibia

The observed spectra are almost identical to each other and very similar to the known spectra of other milarite-type minerals (Downs 2006). Furthermore, there are analogies to vibrational spectra of other silicates containing six-membered rings in their crystal structure, e.g. beryl, indialite or cordierite (e.g. McMillan et al. 1984; Łodziński et al. 2005). Slightly different energies of individual bands arise due to the chemical variations and resulting bonding geometries and strengths. The most pronounced difference among the three spectra in Fig. 3 is the increasing splitting of bands around 550 cm^{-1} in the series milarite-almarudite-friedrichbeckeite, culminating in a clear separation into components with maxima at 577 and 543 cm^{-1} in the latter mineral. Spectra recorded up to 4,000 cm^{-1} yield no evidence for OH, H_2O or other molecular species in friedrichbeckeite and almarudite, whereas milarite shows weak bands due to OH stretching vibrations at ~3,530 cm^{-1}.

Single-crystal X-ray diffraction

Single-crystal intensity data for friedrichbeckeite were collected on a Nonius Kappa goniometer equipped with a CCD area detector, a primary graphite monochromator and a 0.3 mm capillary optics collimator using MoK_α radiation. For data collection, reduction, processing and absorption correction by the multi-scan approach the HKL/HKL-2000 software package (Otwinowski and Minor 1997; Otwinowski et al. 2003) was used. The structure of friedrichbeckeite was refined using the SHELX-97 software (Sheldrick 1997). The bond-valence calculations

were performed using software VALENCE (Brown 1996) with the parameters of Brese and O'Keeffe (1991).

For collecting the used data the whole Ewald sphere up to 30.49 °θ was recorded by the measurement of one φ-and six sets of ω-scans (956 frames with 1° rotation width and 2 x 160 s exposure time/frame), and a crystal to detector distance of 32 mm. After integrating and merging the total of 11529 reflections within the Ewald sphere in space-group *P*1, the resulting 5919 reflections were reduced to a unique dataset of 644 reflections (R_{int} 2.43 %) and 586 reflections with $F_o^2 > 2\sigma$ (F_o^2) by the refinement software. In contrast to almarudite and the milarite from Val Giuf (Armbruster et al. 1989) no forbidden reflections of type (00*l*) with $l \neq 2n$ were observed. Besides that, only 18 non-significant systematic absence violations for space-group symmetry *P*6/*mcc* and no inconsistent equivalents were recorded during the data processing.

The structure refinement was started with the positional parameters of almarudite (Mihajlović et al. 2004) using complex scattering factors (Wilson and Prince 1999) and the crystallographic site labelling according to Forbes et al. (1972). Subsequent difference-Fourier maps gave a clear indication that the *C*-site is almost fully occupied by K (92.6 (8) %), and a partially occupied *B*-site (19.3(6) %) is delocalized along the **c**-axis from the ideal 4*d* coordinates (⅓,⅔,0) to produce a split position with a theoretical maximum occupancy of 50 % and a *B*–*B*' distance of 0.57 (2) Å. As no chemical analysis of the crystal used for data collection was available the scattering factor of Mn was used for Mn + Fe and Mg + Mn were constrained to a full occupancy at the octahedrally coordinated *A*-site. To determine the occupancy at the *T*2-site the sum of Be + Mg was also constrained to a full occupancy. Neither the displacement parameters nor the interatomic distances gave any indication for a chemical substitution of Si by Al at the *T*1-site. The final refinement converged at *R*1 = 3.62 % (w*R*2 = 8.82 %) and the maximum peaks in the final difference-Fourier map were−0.32 and 0.55 eÅ^{-3}. It is noteworthy that no significant electron densities were observed for the *D*-site at (0,0,0). On the basis of this single-crystal work the refined structural formula can be given as $K_{0.93}$ $Na_{0.77}$ ($Mg_{1.61}$ Mn+$Fe_{0.39}$) ($Be_{1.82}Mg_{1.18}$) [$Si_{12}O_{30}$], which agrees well with the results of the chemical analyses. Further details of the data collection, structure refinement and other relevant crystallographic data for friedrichbeckeite are summarized in Table 3, the final positional and displacement parameters are given in Table 4, and selected bond distances and angles within the stereochemical series roedderite-friedrichbeckeite-almarudite-oftedalite in Table 5.

Discussion

The structure of friedrichbeckeite is isotypic to that of milarite and other related minerals (Table 6) with the general structural formula $^{[12]}C$ $^{[9]}B_2$ $^{[6]}A_2$ $^{[4]}T2_3$ [$^{[4]}T1_{12}O_{30}$]. The main feature of their structure (Fig. 4) are [$T1_{12}O_{30}$] units consisting of double six-membered rings of corner-linked

Table 4 Structural parameters for friedrichbeckeite, standard deviations in parentheses

Site	Atom	CN	M	W	*x*	*y*	*z*	U_{eqiv}	Occ.
C	K	[12]	2	*a*	0	0	¼	0.0265(6)	0.926(8)
B	Na	[9]	8	*h*	⅓	⅔	0.0204(7)	0.030(4)	0.193(6)
A	Mg	[6]	4	*c*	⅓	⅔	¼	0.0160(3)	0.807(4)[a]
	Mn[c]								0.193(4)[a]
*T*2	Be	[4]	6	*f*	½	0	¼	0.0114(4)	0.607(4)[b]
	Mg								0.393(4)[b]
*T*1	Si	[4]	24	*m*	0.10056(6)	0.35367(6)	0.10910(3)	0.0123(2)	1
O1	O	[4]	12	*l*	0.1190(3)	0.4085(3)	0	0.0294(5)	1
O2	O	[3]	24	*m*	0.2107(2)	0.2814(2)	0.1284(1)	0.0299(4)	1
O3	O	[4]	24	*m*	0.1353(2)	0.4918(2)	0.1790(1)	0.0222(3)	1

Site	U_{11}	U_{22}	U_{33}	U_{23}	U_{13}	U_{12}
C	0.0242(6)	U_{11}	0.0309(9)	0	0	$U_{11}\times0.5$
B	0.020(3)	U_{11}	0.05(1)	0	0	$U_{11}\times0.5$
A	0.0157(4)	U_{11}	0.0165(6)	0	0	$U_{11}\times0.5$
*T*2	0.0140(7)	0.0059(8)	0.0117(8)	0	0	$U_{22}\times0.5$
*T*1	0.0115(3)	0.0119(3)	0.0132(3)	−0.0021(2)	−0.0002(2)	0.0057(2)
O1	0.047(1)	0.024(1)	0.0124(9)	0	0	0.014(1)
O2	0.0290(8)	0.0393(9)	0.0358(8)	−0.0040(8)	−0.0006(7)	0.0277(8)
O3	0.0304(8)	0.0193(7)	0.0222(7)	−0.0094(5)	−0.0106(6)	0.0164(6)

CN: coordination number, M: site multiplicity, W: Wyckoff letter, U_{eqiv}: equivalent isotropic displacement factor according to Fischer & Tillmanns (1988), Occ.: site occupancy values, U_{ij}: anisotropic displacement factors are defined as exp [$-2\pi^2$ $\Sigma_{i=1}$ $\Sigma_{j=1}$ U_{ij} a_i^* a_j^* h_i h_j]

[a] sum of occupancies was constrained to be 1.0

[b] sum of occupancies was constrained to be 1.0

[c] Mn = Mn + Fe

Table 5 Selected interatomic distances (Å) and angles (°) for friedrichbeckeite and related minerals, standard deviations in parentheses

	Roedderite[a]	Friedrichbeckeite	Almarudite[b]	Oftedalite[c]		Roedderite[a]	Friedrichbeckeite	Almarudite[b]	Oftedalite[c]
C–O2×12	3.057	3.057(2)	3.068	3.047					
B–O1×3	2.491	2.403(3)	2.437		O1–*B*–O1×3	118.5	118.6(1)	118.0	
–O3×3	2.776	2.920(8)	2.93		O3–*B*–O3×3	66.5	67.4(2)	69.6	
–O3′×3	3.270	3.382(8)	3.48		O1–*B*–O3×3	59.5	58.6(1)	58.3	
–*B*’	0.61	0.57(2)	0.69		O3′–*B*–O3′×3	55.5	57.2(2)	57.4	
A–O3×6	2.084	2.122(1)	2.161	2.232	O3–*A*–O3×3	83.3	72.58(8)	70.21	67.9
					O3–*A*–O3×3	89.1	89.27(8)	88.28	87.1
					O3–*A*–O3×6	93.9	99.50(6)	101.21	103.0
					O3–*A*–O3×3	176.1	169.16(8)	168.47	168.0
*T*2–O3×4	1.949	1.715(2)	1.671	1.638	O3–*T*2–O3×2	90.6	94.2(1)	96.06	99.0
					O3–*T*2–O3×2	109.9	108.4(1)	108.59	108.5
					O3–*T*2–O3×2	130.4	127.7(1)	125.14	121.7
*T*1–O3	1.583	1.586(2)	1.591	1.593	O2–*T*1–O2	104.4	103.6(1)	104.01	104.1
–O2	1.621	1.609(2)	1.608	1.608	O1–*T*1–O2	108.9	109.0(1)	109.35	109.7
–O2	1.624	1.610(2)	1.610	1.614	O2–*T*1–O3	109.3	109.7(1)	109.73	109.6
–O1	1.616	1.615(1)	1.612	1.605	O1–*T*1–O2	110.6	110.6(1)	110.81	111.0
mean	1.611	1.605	1.605	1.605	O2–*T*1–O3	113.2	112.4(1)	111.26	110.3
					O1–*T*1–O3	110.3	111.2(1)	111.45	111.8
					*T*1–O1–*T*1	152.7	145.3(2)	143.35	144.9
					*T*1–O2–*T*1	153.1	155.9(1)	156.45	155.5
					*T*1–O3–*T*2	119.7	124.8(1)	126.36	128.2
					*T*1–O3–*A*	141.5	135.82(9)	134.93	133.8
					*T*2–O3–*A*	93.0	96.64(6)	96.86	96.5

[a] Armbruster (1989): values for *P*6/*mcc* calculated from the original description in *P*62*c*

[b] Mihajlović et al. (2004)

[c] Cooper et al. (2006)

Table 6 Crystal-structure data and site-occupancies for milarite-type minerals

	$^{[12]}C$	$^{[9]}B_2$	$^{[6]}A_2$	$^{[4]}T2_3$	$^{[4]}T1_{12}$	*a* [Å]	*c* [Å]	*V* [Å^3]	space-group
Berezanskite [1]	**K**	□	**Ti**	**Li**	**Si**	9.903	14.276	1212.4	$P6_3/mcc$
Friedrichbeckeite	**K**	□, Na	**Mg**, Mn, Fe	**Be**, Mg	**Si**	9.970	14.130	1216.4	*P6/mcc*
Sugilite [2]	**K**	**Na**	**Fe**, Al	**Li**	**Si**	10.009	14.006	1219.5	*P6/mcc*
Almarudite [3]	**K**	□, Na	**Mn**, Fe, Mg	**Be**, Al	**Si**	9.997	14.090	1219.5	*P6/mcc*
Poudretteite [4]	**K**	□	**Na**	**B**	**Si**	10.239	13.485	1224.3	*P6/mcc*
Oftedalite [5]	**K**	□	**Sc**, Ca, Mn	**Be**	**Si**	10.097	13.991	1235.3	*P6/mcc*
Brannockite [2]	**K**	□	**Sn**	**Li**	**Si**	10.002	14.263	1235.7	*P6/mcc*
Sogdianite [6]	**K**	□, Na	**Zr**, Ti, Fe	**Li**	**Si**	10.053	14.211	1243.8	*P6/mcc*
Trattnerite [7]	□, K	□	**Fe**, Mg	**Mg**, Fe	**Si**	10.050	14.338	1254.1	*P6/mcc*
Yagiite [8]	□, K, Na	**Na**	**Mg**	**Al**, Mg, Fe	**Si**, Al	10.09	14.29	1259.9	*P6/mcc*
Osumilite-(Mg) [9]	**K**	□	**Mg**	**Al**	**Si**, Al	10.086	14.325	1262.0	*P6/mcc*
Eifelite [10]	**K**	**Na**	**Mg**, Na	**Mg**	**Si**	10.137	14.223	1265.7	*P6/mcc*
IMA 2007–054[a]	**K**	□, Na	**Fe**	**Zn**	**Si**	10.120	14.298	1268.1	*P6/mcc*
Roedderite [11]	**K**	**Na**, H_2O	**Mg**, Fe	**Mg**, Fe	**Si**	10.141	14.286	1272.6	*P62c*
Osumilite [9]	**K**	□	**Fe**, Mg	**Al**, Fe	**Si**, Al	10.145	14.289	1273.6	*P6/mcc*
Merrihueite [12]	**K**	□, K, Na	**Mg**, Fe	**Mg**, Fe	**Si**	10.16	14.32	1280.2	*P6/mcc*
Chayesite [13]	**K**	□	**Mg**	**Mg**, Fe	**Si**	10.153	14.388	1284.4	*P6/mcc*
Dusmatovite [14]	□, K	**Na**, □	**Mn**, Y, Zr	**Zn**, Li	**Si**	10.218	14.292	1292.6	$P6_3/mcc$
Milarite [15]	**K**	□, H_2O	**Ca**	**Be**, Al	**Si**	10.404	13.825	1296.0	*P6/mcc*
Darapiosite [16]	**K**	**Na**, K, □	**Mn**, Zr, Y	**Li**, Zn, Fe	**Si**	10.262	14.307	1305.0	*P6/mcc*
Shibkovite [17]	**K**	**K**, □	**Ca**, Mn, Na	**Zn**	**Si**	10.505	14.185	1355.7	*P6/mcc*
Armenite [18]	**Ba**	**H_2O**	**Ca**	**Al**	**Si**, Al	10.735[b]	13.874	1384.7[b]	*Pnc2*

References: [1] Pautov and Agakhanov (1997) [2] Armbruster and Oberhänsli (1988b), [3] Mihajlović et al. (2004), [4] Grice et al. (1987), [5] Cooper et al. (2006), [6] Cooper et al. (1999), [7] Postl et al. (2004), [8] Bunch and Fuchs (1969), [9] Armbruster and Oberhänsli (1988a), [10] Abraham et al. (1983), [11] Armbruster (1989), [12] Dodd et al. (1965), [13] Velde et al. (1989), [14] Pautov et al. (1996), [15] Hawthorne et al. (1991), [16] Ferraris et al. (1999), [17] Pautov et al. (1998), [18] Armbruster (1999)

[a] pers. comm. HP Bojar

[b] pseudohexagonal values calculated from the original orthorhombic unit-cell parameters

$T1O_4$-tetrahedra, which are stacked along the **c**-axis, thus establishing a channel system along [0001] with a theoretical effective pore width (Baerlocher et al. 2001) of approximately 2.3 Å. These $[T1_{12}O_{30}]$ units at $z \pm 0,½$ are interconnected by sharing corners with $T2O_4$-tetrahedra at $z \pm ¼,¾$, which, in their turn, are arranged in groups of three around one centrally located AO_6-octahedron to give $[AT2_3]$ units. The subjacent voids at $z \pm 0,½$ located between three $[T1_{12}O_{30}]$ units are represented by the *B*-site, split due to its displacement from the mirror plane at $z = 0,½$. The *C*-site is situated in the centre of the channel between two $[T1_{12}O_{30}]$ units (Fig. 4). The majority of the milarite-group minerals can be described with space-group symmetry *P6/mcc*, which is reduced to *P62c* by Na ordering at the *B*-site in roedderite (Armbruster 1989) or to *Pnc2* by (Al,Si) ordering at the *T*-sites of the double six-membered ring in armenite (Armbruster 1999). The Be:Mg ratio in friedrichbeckeite is ~ 2:1, which could imply a non-statistical (Be,Mg)-distribution at the *T2*-site, i.e. symmetry reduction by cation ordering with the possible end-member K $(□_{0.5}Na_{0.5})_2$ Mg_2 $(Be_{0.66}$ $Mg_{0.33})_3$ $[Si_{12}O_{30}]$. Although no indication of (Be,Mg) ordering was given by the data merging statistics, the structure was tentatively solved and refined in space-group *P*3 with two crystallographically non-equivalent *T2*-sites. Based on the refined (Be,Mg) site occupancy values and *T2*–O distances one can state, that for the crystalline long-range order no deviation from a statistical distribution at any of the five cation positions was detectable. In consistency to the anisotropic displacement parameters of the refinement in *P6/mmc* (Table 4), also no split position for the *A*-site (Hawthorne et al. 1991) was indicated in the low-symmetry refinement. Therefore, it is more likely that the observed ~ 2:1 ratio at the *T2*-site is caused by steric constraints of these differently sized cations from their neighbouring cations in the *A*-and *B*-site.

Due to the chemical variability within the milarite group, a wide range of unit-cell parameters (*a*: 9.90–10.51 Å, *c*: 13.49–14.39 Å) can be observed (Table 6). Consequently, the unit-cell volume varies by ~ 12 vol% between berezanskite and armenite. A plot of *c*:*a* ratios vs. unit-cell volumes is given in Fig. 5, which reveals a significant

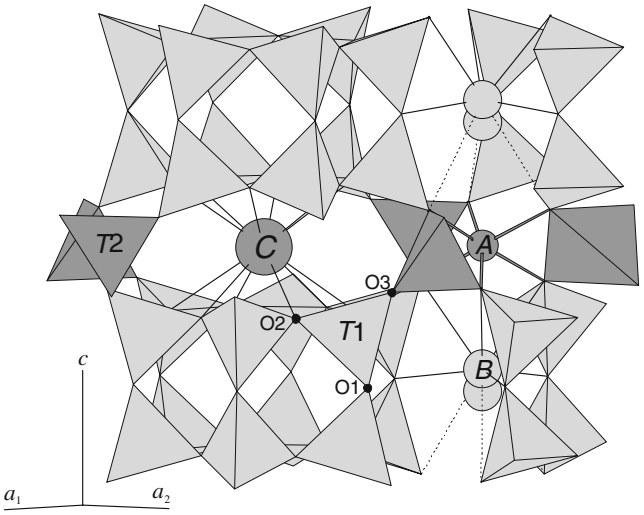

Fig. 4 Representation (Dowty, 2006) of the crystal structure of friedrichbeckeite (viewed approximately along [1$\bar{1}$00]), showing double six-membered rings of *T*1-tetrahedra (light gray) fully occupied by Si and sharing corners with Be-dominated *T*2-tetrahedra (*dark gray*). The edge-sharing, Mg-dominated octahedron is represented by six *A*–O3 bonds. In the partially occupied *B*-site (*light gray sphere*), Na is bonded to 6 + 3 oxygen atoms (*solid and dotted lines*, respectively); the symmetry-related B'-site has a similar bonding configuration (omitted for clarity). The K-dominated *C*-site (*dark gray sphere*) is located between the double six-rings at the centre of the channel; it is bonded to twelve O2 atoms (*solid black lines*)

bimodal *a*:*c* distribution controlled by the size of the cation at the *A*-site, i.e. the stacked $[T1_{12}O_{30}]$ columns are spaced farther apart within the basal plane by large-sized cations. The majority of the milarite-group minerals belongs to the first subgroup with a mean *c*:*a* ratio of 1.41(1), while the four representatives of the second subgroup have a mean *c*:*a* ratio of 1.32(2) and are characterized by the prepon-

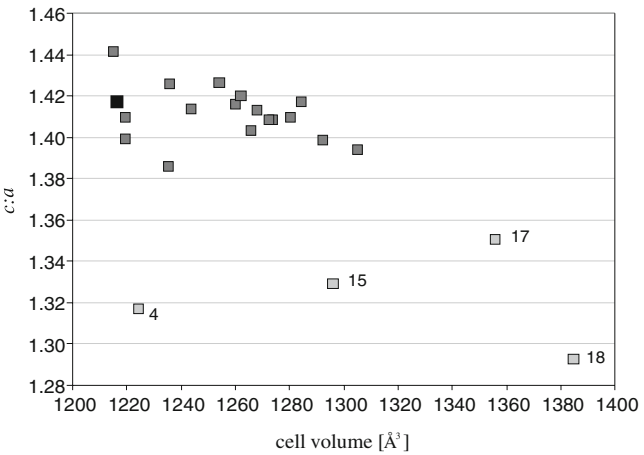

Fig. 5 Plot of the *a*:*c* ratio vs. unit-cell volume of milarite-type minerals based on the data listed in Table 6; Friedrichbeckeite (*black square*); subgroup 1 minerals (*dark grey squares*); subgroup 2 minerals (*light gray squares*); numbers refer to references given in Table 6

derance of Ca and Na at the *A*-site. Friedrichbeckeite with *c*:*a* = 1.417 fits well with the first subgroup and is distinctly different from milarite. The unit-cell volume of friedrichbeckeite is in the lower range of this subgroup, which is dominated by the Li-bearing members (Table 6).

In general, the chemical differences among the milarite-type compounds mainly arise from different substituent elements in the $[AT2_3]$ units, with charge imbalance compensated through substituions at the *B*-site. Consequently, these octahedrally and tetrahedrally coordinated sites exhibit a wide range of interatomic distances pointing out the flexibility of the milarite-type structure. This is also evident from the values given in Table 5 with 1.638 and 1.949 Å for the *T*2–O3 distance (d_{T2}) of oftedalite (*T*2 = $Be_{2.9}Al_{0.1}$) and roedderite (*T*2 = Mg), respectively, both representing the *T*2 end-members of friedrichbeckeite (*T*2 = $Be_{1.8}Mg_{1.2}$) with 1.715(2) Å. Almarudite, with a *T*2-site occupancy of ($Be_{2.2}Al_{0.8}$), has an accordingly shorter d_{T2} of 1.671 Å. This distance value is close to that of milarite sample 33 of Hawthorne et al. (1991), which exhibit an almost identical *T*2-site occupancy and a d_{T2} of 1.669 Å. In contrast to the $T2O_4$-tetrahedron, the *A*–O3 distances (d_A) in oftedalite are larger (A = $Sc_{1.0}Ca_{0.8}Mn_{0.2}$, d_A = 2.232 Å) than in roedderite (A = $Mg_{1.7}Fe_{0.2}Na_{0.1}$, d_A = 2.084 Å) with an increase of the d_A: d_{T2} ratio from 1.07 to 1.36. Friedrichbeckeite (A = $Mg_{1.6}Mn_{0.2}Fe_{0.2}$, d_A: d_{T2} = 1.24) and almarudite (A = $Mn_{1.0}Fe_{0.6}Mg_{0.4}$, d_A: d_{T2} = 1.29) exhibit expectable intermediate values.

A further stereochemical feature is the characteristic distortion of the octahedron and tetrahedron in the $[AT2_3]$ units, with a significant reduction of the length of the shared O3–O3 edges as can be seen from the deviation of the O3–*T*2–O3 angles from the ideal value of 109.47°. For friedrichbeckeite, the length of the shared edges is reduced to 2.512(3) Å, whereas the O3–O3 distance between two successive $[T1_{12}O_{30}]$ units is enlarged to 3.079(3) Å. Additionally, it is obvious from the data that for both polyhedra a positive correlation between the degree of polyhedral distortion and mean cation size exists, which can be attributed to the relatively inflexible behaviour of the single six-membered silicate rings parallel to the basal plane, resulting in a nearly constant *T*1–O2–*T*1 angle of 156°. One can conclude that, besides the polyhedral distortion, the stereochemical influence of the different substituent elements at the *A*- and *T*2-sites of the milarite-type structure is compensated by the ring-connecting *T*1–O1–*T*1 angles and the corner-linkage between the $[T1_{12}O_{30}]$ and $[AT2_3]$ units via the *T*1–O3–*T*2 and *T*1–O3–*A* angles. For friedrichbeckeite, the respective values are in good agreement with the established trends (Table 5).

The bond-valence sums were calculated for the cations and anions in friedrichbeckeite taking into account the mixed occupancies of the *A*- and *T*2-site, and the partial

occupancies of the *C*- and *B*-site (Table 4). The obtained values are 0.92 (*C*), 0.15 (*B*), 1.98 (*A*), 2.25 (*T*2), 4.18 (*T*1), 2.08 (O1), 2.14 (O2) and 1.99 (O3) valence units (v.u.), which agree with the observed substitutions in the *A*- and *T*2-sites. The values also reflect that the *C*-and *B*-sites are not fully occupied as a fully occupied *B*-site would result in an oversaturation at the O1-site. Somewhat high values for the *T*2- and *T*1-site were also reported for almarudite (*C*: 0.88, B: 0.03, *A*: 2.03, *T*2: 2.34, *T*1: 4.21, O1: 2.13, O2: 2.16, O3: 2.02 v.u.) by Mihajlović et al. (2004), although, in this case one has to take into account the presence of Al at the *T*2-site. The pale colour of fridrichbeckeite indicates the $Mg^{2+} \leftrightarrow Fe^{3+}$ substitution is unlikely in the studied material. The bond-valence sums calculated for the oxygen atoms compare well with those of almarudite and synthetic merrihueite (Khan et al. 1972) including the characteristically lower valence state of O3.

As mentioned before, the most pronounced difference between the Raman spectra of friedrichbeckeite and related minerals (Fig. 3) is the increasing splitting of the scattering bands at 550 cm^{-1} in milarite and almarudite into separate components with maxima at 577 and 543 cm^{-1} in friedrichbeckeite. As the Raman bands predominantly reflect the short-range order characteristics, this may be a consequence of the increased distortion of the *T*2-tetrahedron, which is less distorted in milarite (Hawthorne et al. 1991: O3–*T*2–O3 = 102.9, 109.6, 116.2°) than in oftedalite or almarudite (Table 5). Alternatively, the chemical differences between these minerals, or local order/disorder phenomena (as reported for cordierite by Poon et al. 1990) may be related to the observed splitting. Thus, the results of the X-ray diffraction study are not in contradiction with these observations. The crystal-chemical features of the milarite-group minerals, involving various substitutions at the cation sites and the presence of vacancies at the *B*-site, causes the complexity of the spectra, preventing a detailed interpretation of individual bands. The prominent bands in the region 1,200–900 cm^{-1} can be interpreted as internal stretching vibrations of *T*1-tetrahedra, whereas the multitude of bands below 900 cm^{-1} can be attributed to O–*T*–O and *T*–O–*T* bending modes, complex vibrations of the silicate rings, as well as coinciding bands originating from the [$AT2_3$] unit and lattice modes at the very low energy end of the spectrum (e.g. McMillan et al. 1984; Łodziński et al. 2005). However, a more detailed discussion of the Raman spectra is beyond the scope of the present paper.

Identification and classification

The appearance, tabular habit and light yellow colour of friedrichbeckeite are similar to those of the other isotypic Mg dominated milarite-type minerals from the Bellerberg locality (Hentschel 1987), the refractive indices of friedrichbeckeite, however, are significantly higher than for the eifelite–roedderite series (Abraham et al. 1983: n_ω = 1.543–1.545, n_ε = 1.545–1.547). Almarudite, on the other hand, exhibits a more vivid yellow to orange colour and is optically negative, whereas osumilite is also optically negative, but distinctly blue in colour (Schreyer et al. 1983). Another potentially diagnostic property is the relatively small volume of friedrichbeckeite, although a detailed chemical analysis will be necessary for unambiguous identification.

Based on the six-membered double-ring as the main structural feature, friedrichbeckeite can be categorized as an unbranched ring silicate (Liebau 1985) or, with respect to the substituent elements at the *T*-sites, as a beryllo-magnesiosilicate. The polyhedral topology of this structure type, as pointed out by Hawthorne et al. (1991), can be classified as a $(4^26^4)_4(6^49^2)$ framework (Hawthorne and Smith 1986) with a close structural relationship to other ring silicates like beryl and indialite. For a further subdivision within the group of isotypic milarite-type minerals (Table 6) the end-member formula K $(\square_{0.5}Na_{0.5})_2$ Mg_2 Be_3 $[Si_{12}O_{30}]$ of friedrichbeckeite can be considered as the Mg-analogue of almarudite, K $\square_2$ Mn_2 $(Be_{0.66}Al_{0.33})_3$ $[Si_{12}O_{30}]$, milarite, K $\square_2$ Ca_2 $(Be_{0.66}Al_{0.33})_3$ $[Si_{12}O_{30}]$ or oftedalite, K $\square_2$ $(Sc_{0.5}Ca_{0.5})_2$ Be_3 $[Si_{12}O_{30}]$. Following Hawthorne (2002) the divalent state of the cations at the *A*- and *T*2-sites and their charge-compensation by Na at the *B*-site may be taken into consideration, and friedrichbeckeite may be regarded as the Be-analogue of merrihueite, K $(K_{0.5}\square_{0.5})_2Mg_2$ Mg_3 $[Si_{12}O_{30}]$, or roedderite, K $(Na_{0.5}\square_{0.5})_2$ Mg_2 Mg_3 $[Si_{12}O_{30}]$.

Acknowledgements The authors thank J. Jahn (Neuwied, Germany) for providing the material studied in the present paper, M. Wagner for sample preparations as well as T. Ntaflos, U. Klötzli, M. A. Götzinger and G. Giester (all Wien, Austria) for their support with the chemical microanalyses and single-crystal X-ray diffraction. The useful comments of CNMNC members and the detailed suggestions of M. Cooper (Winnipeg, Canada) and an anonymous reviewer as well as the considerable improvements of the Associate Editor A. Chakhmouradian (Winnipeg, Canada) are gratefully acknowledged. The work was supported by the International Centre for Diffraction Data through Grant 90–03.

References

Abraham K, Gebert W, Medenbach O, Schreyer W, Hentschel G (1983) Eifelite, $KNa_3Mg_4Si_{12}O_{30}$, a new mineral of the osumilite group with octahedral sodium. Contrib Mineral Petrol 82:252–258

Armbruster T (1989) Crystal chemistry of double-ring silicates: structure of roedderite at 100 and 300 K. Eur J Mineral 1:715–718

Armbruster T (1999) Si, Al ordering in the double-ring silicate armenite, $BaCa_2Al_6Si_9O_{30}{\cdot}2H_2O$: A single-crystal X-ray and ^{29}Si MAS NMR study. Am Mineral 84:92–101

Armbruster T, Bermanec V, Wenger M, Oberhänsli R (1989) Crystal chemistry of double-ring silicates: structure of natural and dehydrated milarite at 100 K. Eur J Mineral 1:353–362

Armbruster T, Oberhänsli R (1988a) Cystal chemistry of double-ring silicates : Structural, chemical and optical variation in osumilites. Am Mineral 77:585–594

Armbruster T, Oberhänsli R (1988b) Crystal chemistry of double-ring silicates: Structures of sugilite and brannockite. Am Mineral 73:595–600

Baerlocher C, Meier WM, Olson DH (2001) Atlas of zeolite framework types, 5th Ed. Elsevier, Amsterdam, The Netherlands, p 302

Becke F (1892) Petrographische Studien am Tonalit des Rieserferner. Tschermaks Mineral Petrogr Mitth 13:379–430 cf. p 386

Bogaard P, Schmincke H-U (1990) Die Entwicklungsgeschichte des Mittelrheinraumes und die Eruptionsgeschichte des Osteifel-Vulkanfeldes. In: Schirmer W (ed) Rheingeschichte zwischen Mosel und Maas. Deuqua Führer, 1. Hannover, Germany, pp 166–190

Brese NE, O'Keeffe M (1991) Bond-valence parameters for solids. Acta Crystallogr B47:192–197

Brown ID (1996) VALENCE: a program for calculating bond valences. J Appl Crystallogr 29:479–480

Bunch TE, Fuchs LH (1969) Yagiite, a new sodium-magnesium analogue of osumilite. Am Mineral 54:14–18

Černý P, Hawthorne FC, Jarosewich E (1980) Crystal chemistry of milarite. Can Mineral 18:41–57

Chester AH (1896) A dictionary of the names of minerals including their history and etymology. Wiley and Sons, New York, p 320

Cooper MA, Hawthorne FC, Ball NA, Černý P, Kristiansen R (2006) Oftedalite, (Sc, Ca, Mn^{2+}) $_2$ K (Be, Al) $_3$ $Si_{12}O_{30}$, a new member of the milarite group from the Heftetjern pegmatite, Tørdal, Norway: Description and crystal structure. Can Mineral 44:943–949

Cooper MA, Hawthorne FC, Grew ES (1999) The crystal chemistry of sogdianite, a milarite-group mineral. Am Mineral 84:764–768

Dodd RT, van Schmus WR, Marvin UB (1965) Merrihueite, a new alkali-ferromagnesian silicate from the Mezö-Madaras chondrite. Science 149:972–974

Downs RT (2006) The RRUFF Project: An integrated study of the chemistry, crystallography, Raman and infrared spectroscopy of minerals. Program and Abstracts of the 19th General Meeting of the International Mineralogical Association in Kobe, Japan, O03–13

Dowty E (2006) ATOMS: A computer program for displaying atomic structures. Kingsport TN 37663, USA

Embrey PG, Fuller JP (1980) A manual of new mineral names 1892–1978. Oxford University Press, New York, p 467

Ferraris G, Prencipe M, Pautov LA, Sokolova EV (1999) The crystal structure of darapiosite and a comparison with Li-and Zn-bearing minerals of the milarite group. Can Mineral 37:769–774

Fischer RX, Lengauer CL, Tillmanns E, Ensink RJ, Reiss CA, Fantner EJ (1993) PC-Rietveld plus, a comprehensive Rietveld analysis package for PC. Mater Sci Forum 133–136:287–292

Fischer RX, Tillmanns E (1988) The equivalent isotropic displacement factor. Acta Crystallogr C44:775–776

Forbes WC, Baur WH, Khan AA (1972) Crystal chemistry of milarite-type minerals. Am Mineral 57:463–472

Gandolfi G (1964) Metodo per ottenere uno spettro di polveri da un cristallo singolo di piccole dimensioni (fino a 30μ). Mineral. Petrogr. Acta 10:149–156

Grice JD, Erict TS, Van Velthuizen J, Dunn PJ (1987) Poudretteite, $KNa_2B_3Si_{12}O_{30}$, a new member of the osumilite group from Mont Saint-Hilaire, Quebec, and its crystal structure. Can Mineral 25:763–766

Hawthorne FC (2002) The use of end-member charge-arrangements in defining new mineral species and heterovalent substitutions in complex minerals. Can Mineral 40:699–710

Hawthorne FC, Kimata M, Černý P, Ball N, Rossman GR, Grice JD (1991) The crystal chemistry of the milarite-group minerals. Am Mineral 76:1836–1856

Hawthorne FC, Smith JV (1986) Enumeration of 4-connected 3-dimensional nets and classification of framework silicates. 3D nets based on insertion of 2-connected vertices into 3-connected plane nets. Z Kristallogr 175:15–30

Hentschel G (1987) Die Mineralien der Eifelvulkane, 2nd Ed. Weise, München, Germany, p 177

Hrauda N (2006) Manganführende Minerale der Osumilithgruppe aus dem Eifelgebiet. Diploma thesis, Universität Wien, Wien, p 104

Irran E, Tillmanns E, Hentschel G (1997) Ternesite, $Ca_5(SiO_4)_2(SO_4)$, a new mineral from the Ettringer Bellerberg, Eifel, Germany. Mineral Petrol 60:121–132

Khan AA, Baur WH, Forbes WC (1972) Synthetic magnesian merrihueite, dipotassium pentamagnesium dodecasilicate: a tetrahedral magnesiosilicate framework crystal structure. Acta Crystallogr B28:267–272

Krause W, Blass G, Effenberger H (1999) Schäferite, a new vanadium garnet from the Bellberg volcano, Eifel, Germany. N Jb Mineral Mh 1999:123–134

Liebau F (1985) Structural chemistry of silicates. Springer, Berlin, Germany, p 347

Łodziński M, Wrzalik A, Sitarz M (2005) Micro-Raman spectroscopy studies of some accessory minerals from pegmatites of the Sowie Mts and Strzegom-Sobótka massif, Lower Silesia, Poland. J Mol Str 744–747:1017–1026

Mandarino JA (1981) The Gladstone-Dale relationship: Part IV. The compatibility concept and its application. Can Mineral 19:441–450

McMillan P, Putnis A, Carpenter M (1984) A Raman spectroscopic study of Al-Si ordering in synthetic magnesium cordierite. Phys Chem Minerals 10:256–260

Meyer W (1994) Geologie der Eifel, 3rd Ed. Schweizerbart, Stuttgart, Germany, p 618

Mighell AD, Hubbard CR, Stalick JK (1981) NBS*AIDS83: A FORTRAN program for crystallographic data evaluation. NBS Technical Note 1141

Mihajlović T, Lengauer CL, Ntaflos T, Kolitsch U, Tillmanns E (2004) Two new minerals, rondorfite, $Ca_8Mg[SiO_4]_4Cl_2$, and almarudite, K(□, Na) $_2$(Mn, Fe, Mg) $_2$(Be, Al) $_3$[$Si_{12}O_{30}$], and a study on iron-rich wadalite, $Ca_{12}[(Al_8Si_4Fe_2)\ O_{32}]Cl_6$, from the Bellerberg (Bellberg) volcano, Eifel, Germany. N Jb Mineral Abh 179:265–294

Otwinowski Z, Borek D, Majewski W, Minor W (2003) Multi-parametric scaling of diffraction intensities. Acta Crystallogr A59:228–234

Otwinowski Z, Minor W (1997) Processing of X-ray diffraction data collected in oscillation mode. Methods in Enzymology Series Vol 276: Macromolecular Crystallogr A 307–326 (Carter CW, Sweet RM Eds.), Academic, San Diego

Pautov LA, Agakhanov AA (1997) Berezanskite, $KLi_3Ti_2Si_{12}O_{30}$, a new mineral. Zap Vseross Mineral Obshch 126(4):75–80

Pautov LA, Agakhanov AA, Sokolova EV (1998) Shibkovite K(Ca, Mn, Na) $_2$(K_2-x□x) $Zn_3Si_{12}O_{30}$-a new mineral of the milarite group. Zap Vseross Mineral Obshch 127(4):89–94

Pautov LA, Agakhanov AA, Sokolova EV, Ignatenko KI (1996) Dusmatovite a new mineral of the milarite group. Vestnik Moscov Univ, Ser 4 Geol (2):54–60

Poon WCK, Putnis A, Salje E (1990) Structural states of Mg cordierite: IV. Raman spectroscopy and local order parameter behaviour. J Phys Condens Matter 2:6361–6372

Postl W, Walter F, Ettinger K, Hauzenberger C, Bojar HP (2004) Trattnerite, (Fe, Mg) $_2$(Mg, Fe) $_3$[$Si_{12}O_{30}$], a new mineral of the

milarite group: mineral data and crystal structure. Eur J Mineral 16:375–380

Rüdinger B, Tillmanns E, Hentschel G (1993) Bellbergite-a new mineral with the zeolite structure type EAB. Mineral Petrol 48:147–152

Schreyer W, Hentschel G, Abraham K (1983) Osumilith in der Eifel und die Verwendung dieses Minerals als petrogenetischer Indikator. Tschermaks Mineral Petrogr Mitt 31:215–234

Sheldrick GM (1997) SHELXS-97 and SHELXL-97. Universität Göttingen, Göttingen, Germany

Straumanis M, Jevinš A (1936) Präzisionsaufnahmen nach dem Verfahren von Debye und Scherrer. II. Z Physik 98:461–475

Velde D, Medenbach O, Wagner C, Schreyer W (1989) Chayesite, K (Mg, Fe_2^{+}) $_4Fe_3^{+}$ [$Si_{12}O_{30}$]: A new rock forming silicate mineral of the osumilite group from the Moon Canyon (Utah) lamproite. Am Mineral 74:1368–1373

Wilson AJC, Prince E (1999) International tables for crystallography, vol C. Mathematical, physical and chemical tables. 2nd Ed, Kluwer, Dordrecht, The Netherlands, 992 pp

Winter W, Armbruster T, Lengauer CL (1995) Crystal structure refinement of synthetic osumilite-type phases: $BaMg_2Al_6Si_9O_{30}$, $SrMg_2Al_6Si_9O_{30}$ and $Mg_2Al_4Si_{11}O_{30}$. Eur J Mineral 7:227–286

Winter W, Berger A, Müller G, Pannhorst W (1993) Crystallization mechanism of MAS osumilite with composition $Mg_2Al_4Si_{11}O_{30}$ from glass. J Am Ceram Soc 76:1837–1843